Stimulated Emission of Fast Alfvén Waves within Magnetically Confined Fusion Plasmas

J. W. S. Cook,[1,2,*] R. O. Dendy,[3,1] and S. C. Chapman[1]
[1]Centre for Fusion, Space and Astrophysics, Department of Physics, Warwick University, Coventry CV4 7AL, United Kingdom
[2]First Light Fusion Ltd., Unit 10, Oxford Industrial Park, Yarnton OX5 1QU, United Kingdom
[3]CCFE, Culham Science Centre, Abingdon, Oxfordshire OX14 3DB, United Kingdom
(Received 24 May 2016; revised manuscript received 31 October 2016; published 4 May 2017)

A fast Alfvén wave with a finite amplitude is shown to grow by a stimulated emission process that we propose for exploitation in toroidal magnetically confined fusion plasmas. Stimulated emission occurs while the wave propagates inward through the outer midplane plasma, where a population inversion of the energy distribution of fusion-born ions is observed to arise naturally. Fully nonlinear first-principles simulations, which self-consistently evolve particles and fields under the Maxwell-Lorentz system, demonstrate this novel "α-particle channeling" scenario for the first time.

DOI: 10.1103/PhysRevLett.118.185001

There is overwhelming evidence for the natural occurrence of a substantial inversion in the energy distribution of fusion-born ions at the outer midplane edge of large tokamak plasmas. Spontaneous relaxation of this population is observed in the form of intense (emissive power $\sim 10^4$ times that of a blackbody at the same plasma temperature [1]) suprathermal ion cyclotron emission (ICE), resulting from the excitation of waves on the fast Alfvén branch by means of the collective magnetoacoustic cyclotron instability (MCI) [2–10]. These waves are primarily electromagnetic, with an electrostatic component, and are observed at narrow spectral peaks at frequencies of tens or hundreds of megahertz, corresponding to local sequential ion cyclotron harmonics. For the unique deuterium-tritium (DT) plasmas [11–13], the energy-inverted ion population driving the MCI comprises a subset of the centrally born trapped fusion products, lying just inside the trapped-passing boundary in velocity space, whose drift orbits make large radial excursions to the outer midplane edge [14]. These energetic ion orbits are plotted in Fig. 14 of Ref. [11]; see also Figs. 15 and 16. In other large magnetically confined fusion (MCF) plasmas, an analogous energetic ion population can arise from neutral beam injection or trace fusion reactions. For example, ICE is detected at the edge cyclotron harmonics of the proton, triton, and ^{3}He products of fusion reactions in pure deuterium plasmas [15–18]. ICE is also used as a diagnostic of lost fast ions [19–21]. Recent first-principles simulations [22,23] exploiting particle-in-cell and hybrid kinetic-fluid codes indicate that observed ICE can grow from noise into the nonlinear saturated regime on the fast time scales of relevance. These simulations further confirm the physics assumptions made in analytical studies [3–10] of the MCI for ICE interpretation. Thus, the combination of high temperature plasma conditions with toroidal magnetic confinement geometry leads naturally to a spatially localized source of spontaneous collective emission of spectrally structured electromagnetic waves with strongly suprathermal intensity.

In this Letter, we propose and investigate, for the first time, a stimulated emission counterpart to the observed spontaneous emission process. We use "stimulated emission" in its textbook sense: energetic ions form a spatially localized population inversion; a naturally unstable mode of the system is introduced; and it grows rapidly owing to collective relaxation of the inverted population, on a time scale faster than the spontaneous decay. The simulations reported below show that $\sim 15\%$ of the energy stored in the minority energetic α-particle population, $\epsilon_{\alpha 0}$, can be transferred to an imposed fast Alfvén wave on time scales between $2\tau_{c\alpha}$ and $5\tau_{c\alpha}$, for initial wave energies ranging from $10^{-2}\epsilon_{\alpha 0}$ to $10^{-6}\epsilon_{\alpha 0}$. The magnitude of the eventual increase in wave energy is found to be independent of the imposed wave energy.

These proof-of-principle results indicate that stimulated emission of inward propagating fast Alfvén waves in the edge region may become a significant addition to the techniques for α channeling in MCF plasmas. α channeling [24–26] denotes the exploitation of the free energy in fusion-born ions to, for example, drive internal currents [27–29], radially transport and cool resonant particles [24,26,30], and, preferentially, heat fuel ions [31,32]. This is in contrast to conventional α-particle heating of the thermal plasma by collisions with electrons. A variety of α-channeling mechanisms have been studied, typically involving (as in the novel case proposed here) fast collective relaxation and radiation. There are various potential α-channeling applications of a fast Alfvén wave

originating from stimulated emission by fusion-born ions at the outer midplane edge of MCF plasmas. The additional fuel-ion kinetic energy is initially in the form of coherent oscillation supporting the stimulated fast Alfvén wave; this energy can be thermalized through collisions. Also, ion cyclotron resonant damping of the amplified wave deeper within the plasma would by-pass the lossy electron channel. This process could also extend the use of ICE as a diagnostic for fusion-born ion populations in future DT plasmas in JET and ITER, as proposed in Refs. [33,34]. ICE occurs in solar-terrestrial and, probably, astrophysical plasmas [35–38], suggesting that stimulated emission of fast Alfvén waves, by the mechanism investigated here, could also arise in those natural plasma contexts.

An efficient α-channeling scenario could combine the mechanism reported here with that of Herrmann and Fisch [26], from which similar population inversions may arise containing $\lesssim$30% of the total number of α particles: Alfvén eigenmodes nudge α particles in the plasma core onto drift orbits of the inverted population, from which stimulated emission extracts energy.

We deploy the relativistic one spatial and three velocity–dimension (1D3V) particle-in-cell (PIC) code EPOCH [39] to self-consistently integrate the electromagnetic field simultaneously with the fully kinetic distributions of electrons, deuterons, and α particles. Initially, electrons and majority fuel-ion deuterons are thermalized at 1 keV, and the minority fusion-product α particles exhibit a ring distribution in velocity space, $f(v_\perp, v_\parallel) \propto \delta(v_\perp - u_\perp)\delta(v_\parallel)$, where $v_\parallel \equiv v_z$, $v_\perp^2 = v_x^2 + v_y^2$, and $u_\perp$ corresponds to the speed of 3.5 MeV. All three components of field and velocity vectors may vary in one direction, x, in this Maxwell-Lorentz system, and a uniform magnetic field of 2.1 T is initialized along the z axis. The electron density is 10^{19} m^{-3} and the ratio of the α-particle density to the deuteron density is 10^{-3}. This is an order of magnitude higher than in experiments [1,11], and it is chosen to raise the signal above the noise. Each species is represented by 200 particles per cell, with a total of 4096 cells. Presented below are results from a parameter scan in energy of an imposed fast Alfvén wave. This energy is varied from 1% of that initially in the α-particle population in steps of factors of 10 down to 10^{-8}. In this preliminary study, the fast Alfvén wave has a frequency of $18\omega_{c\alpha}$, and we set the periodic simulation domain length to 120 wavelengths. This frequency is one at which the MCI grows in the absence of any imposed waves, and it is within the range of frequencies that are routinely injected at high power (up to several megawatts) to drive currents within plasmas [39]. Perturbed quantities and the wave number are determined by the cold plasma dispersion relation [40] at this frequency. The imposed wave perturbs the electric field components such that

$$\begin{bmatrix} S - n^2 & -iD \\ iD & S - n^2 \end{bmatrix} \begin{bmatrix} E_x \\ E_y \end{bmatrix} = \begin{bmatrix} 0 \\ 0 \end{bmatrix}, \quad (1)$$

where S, D, and the perpendicular refractive index n are defined in Ref. [40]. This linear cold plasma wave is an approximation to the nonlinear hot plasma wave represented in the fully kinetic PIC code that we deploy [41]. The wave is initialized in the simulation with coherent spatial perturbations to the B_z, E_x, and E_y fields, J_x and J_y current components, bulk v_x and v_y components of the velocity of electrons and deuterons, and the electron and deuteron densities. The α particles are initially unperturbed. Maxwell's equations and the conservation of mass and momentum determine the perturbed quantities at initialization time. Thus, the imposed wave is a self-consistent solution of the system of equations solved by the PIC code and is initially supported by the majority deuteron and electron populations only. Thereafter, the evolution of the perturbed fields and particles, including the α particles, is governed self-consistently by the PIC solver [41]. These simulations present an idealized scenario where α particles, in the absence of particle sources or sinks, initially have an infinitely narrow distribution function and no spatial inhomogeneities.

Electrons and deuterons are initialized with the quiet start method used in Refs. [22,28]. The computational macroparticles are initialized uniformly in configuration space and randomly in velocity space so that their distributions approximate the initial conditions. The cell-integrated first and second moments of the distribution functions are used to correct the particle velocities to match the initial conditions exactly on a cell averaged basis. The α particles are initialized uniformly in configuration space and quasiuniformly in gyro angle, such that spatially adjacent particles in each cell have opposing velocities. On a cell averaged basis, the α-particle charge density is uniform and the cell summed current is zero; hence, our initial conditions are satisfied exactly.

Figure 1 shows the temporal evolution of the normalized change in the energy density of the deuteron and α-particle populations, averaged across the simulation domain. Increasing the amount of energy in the applied wave causes energy to be extracted faster from the α-particle population and deposited in the deuterons whose coherent oscillations support the linearly [7] and nonlinearly [23] excited waves. Importantly, much of this energy is passed to the majority thermal deuterons; see Fig. 1. Hence, we have identified a new method for collisionless energy transfer from fusion product α particles to fusion fuel ions. The increased kinetic energy of the deuterons is a direct transfer of energy into low entropy coherent oscillations; subsequent collisions on longer time scales would randomize this motion, thereby increasing the deuterons' entropy and temperature. This form of direct fuel-ion energization is of particular interest since it reduces the fraction of fusion energy wasted in heating the electrons. Additionally, the negative group speed of the amplified imposed fast Alfvén wave implies energy transfer towards the plasma core.

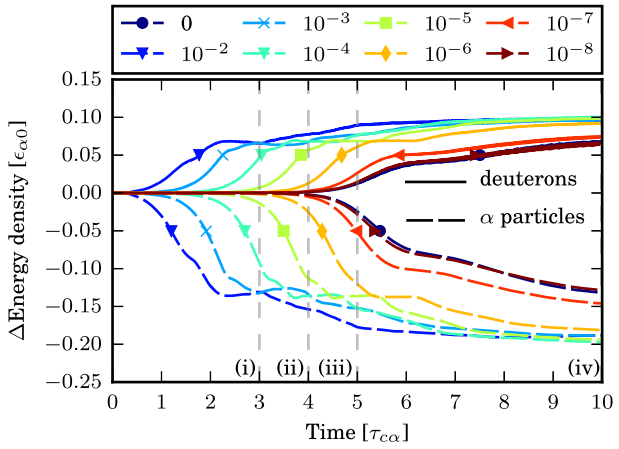

FIG. 1. Stimulated emission of 10%–20% of the energy of the α-particle population over a few gyroperiods, when subjected to resonant fast Alfvén waves that have much lower energy density. Temporal evolution of the minority α-particle population energy density (the dashed traces) and deuteron energy density (the solid traces) in response to applied waves with a range of energy densities. Marked pairs of traces for α particles and deuterons show energy change in the presence of waves with energy densities ranging between 10^{-2} and 10^{-8} that of the energy initially in the α particles, and the null case, labeled 0, without an imposed wave. Energetic minority α particles transfer energy to thermal majority deuterons on shorter time scales when subjected to higher amplitude fast Alfvén waves. The eventual level of energy transfer is broadly the same. Vertical dashed lines annotated (i)–(iv) indicate the snapshots in time displayed in Fig. 4. The change in energy density (the ordinate) is plotted in units of the initial α-particle energy density $\epsilon_{\alpha 0}$, and the time (the abscissa) is plotted in units of the α-particle cyclotron time period $\tau_{c\alpha} = 2\pi/\omega_{c\alpha}$.

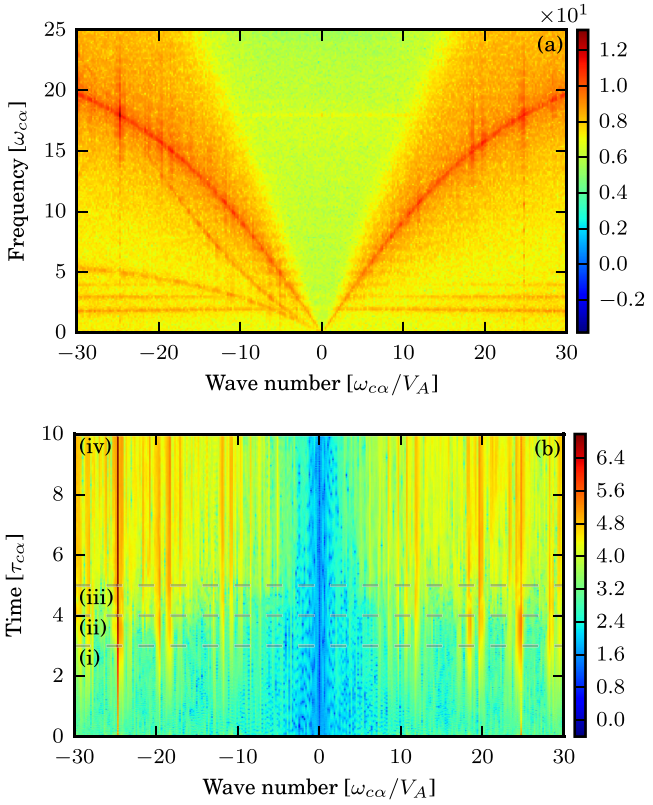

FIG. 2. Dominant waves, and their linear and nonlinear interactions, identified from Fourier transforms of the computed E_x field in the simulations. These are obtained by computing the fast Fourier transform of the whole spatial and temporal domain from a simulation with an imposed Alfvén wave with an initial energy of $10^{-5}\epsilon_{\alpha 0}$. (a) (ω, k) amplitudes. (b) (t, k) amplitudes.

Figure 2(a) plots the power in the spatiotemporal fast Fourier transform of the electric field component aligned with the grid, E_x, integrated over the whole spatial and temporal domain. Notable peaks in the spectrum are located at the frequency and wave number of the imposed wave $(\omega_i = 18\omega_{c\alpha},\ k_i \simeq -25\omega_{c\alpha}/V_a)$, frequencies and wave numbers of oppositely traveling waves to which the imposed wave couples $(14 \lesssim \omega/\omega_{c\alpha} \lesssim 20,\ 18 \lesssim kV_A/\omega_{c\alpha} \lesssim 30)$, and the first harmonic of the imposed wave (ω=$36\omega_{c\alpha}$, $k \simeq -50\tau_{c\alpha}/V_a$) (not shown). Figure 2(b) plots the power in E_x as a function of the time and the signed wave number. Undulations in time are visible at constant wave number, indicating the onset of nonlinearity in the forward propagating waves $(3 \lesssim t/\tau_{c\alpha} \lesssim 4,\ 18 \lesssim kV_A/\omega_{c\alpha} \lesssim 30)$, which couple to the imposed wave. Referring to Fig. 1, this matches the end of the linear phase of the instability.

The extracted energy travels through the plasma at the wave packet's group speed, which in a hot plasma is analytically inaccessible; see Eq. (69) in Ref. [3]. The simulations enable us to measure it in Fig. 3, which shows the spatiotemporal evolution of wave packets of the imposed wave with frequency and wave number (ω_i, k_i) in the E_x field [Fig. 3(a)] and the α-particle number density [Fig. 3(b)]. Shading shows the absolute value of a wavelet analysis, which consists of a windowed discrete Fourier transform (DFT) at the imposed frequency and wave number (ω_i, k_i). The wavelet DFT, of spatiotemporal extent $2\pi(|k_i^{-1}|, \omega_i^{-1})$, is applied periodically in the spatial direction and aperiodically in the temporal. Each instantaneous application of the wavelet DFT adds to the value at any (x, t) position that its window overlaps. Figure 3(a) confirms that the energy in the imposed wave travels from right to left at $(1.0 \pm 0.2)v_{gi}$, where v_{gi} is the group speed of the imposed wave implicitly defined by Eq. (1). This velocity corresponds to $(-0.40 \pm 0.06)V_A \simeq (0.55 \pm 0.08)\omega_i/k_i$, where $k_i < 0$. In a tokamak, the energy of a wave launched from the outboard edge would be amplified by α-particle energy and would travel further towards the core at the wave's group speed. Figure 3(b) indicates the abrupt start, at $t \simeq 4\tau_{c\alpha}$, of the nonlinear phase in the α-particle spatial distribution at the imposed wave's wave number and frequency (cf. the dashed trace labeled 10^{-5} in Fig. 1).

Our fully kinetic 1D3V simulations give a detailed view of the temporal evolution of perturbations to the α-particle

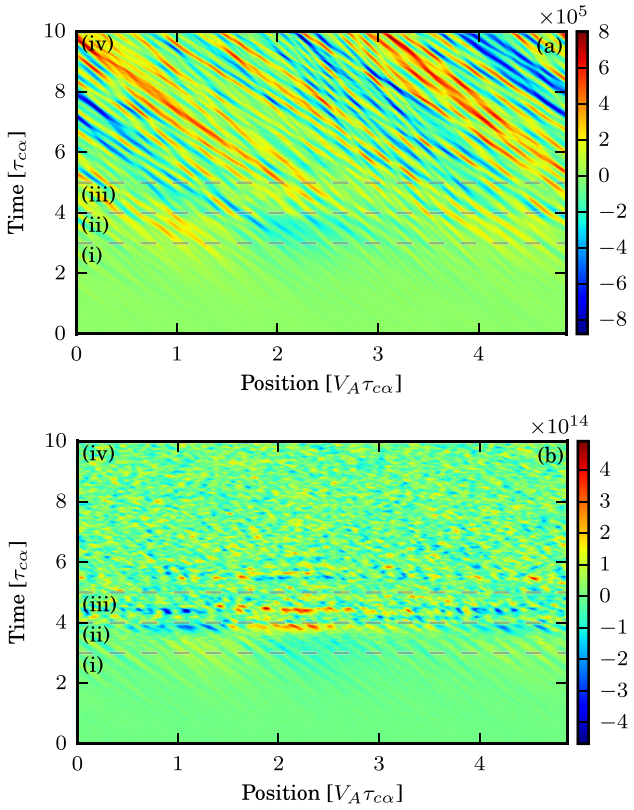

FIG. 3. Coherent field oscillations persist through, and beyond, the sudden transition to strong nonlinearity in α-particle dynamics. Linear (early time) and nonlinear (late time) propagation and evolution of energy wave packets at the imposed frequency ω_i and wave number k_i. Shading indicates the spatiotemporal amplitude of the 2D wavelet DFT at (ω_i, k_i) of (a) the E_x field and (b) the α-particle number density for a wavelet window of the size $2\pi(\omega_i^{-1}, |k_i^{-1}|)$ (see the text). Data are from the simulation shown in Fig. 2.

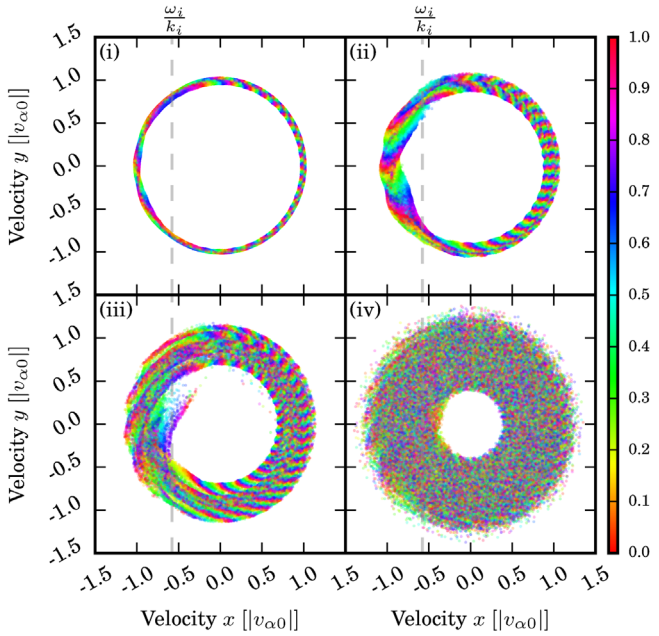

FIG. 4. Sudden transition to nonlinear α-particle dynamics at $t \simeq 4\tau_{c\alpha}$. Linear and nonlinear wave-particle interactions shown in the perpendicular velocity space of a randomly selected sample of 10% of α particles at four times, (i)–(iv), which are marked in Figs. 1–3. Shading represents the value of x modulo $2\pi/k_i$ at $t = 3\tau_{c\alpha}$, $4\tau_{c\alpha}$, $5\tau_{c\alpha}$, and $10\tau_{c\alpha}$. The dashed vertical trace shows the phase speed of the imposed fast Alfvén wave, ω_i/k_i. Velocity is in units of the initial α-particle speed, $v_{\alpha 0}$. Data are from the same simulation shown in Figs. 2 and 3.

distribution function. Figure 4 plots the perpendicular components of velocity, v_x and v_y, of the α particles, where shading shows the value of x modulo $2\pi/k_i$ at four snapshots in time: Fig. 4(i) shows the imprint of the MCI during the linear stage of the process at $3\tau_{c\alpha}$; Figs. 4(ii) and 4(iii) show the nonlinear development at $4\tau_{c\alpha}$ and $5\tau_{c\alpha}$, respectively; and Fig. 4(iv) shows the final state at $10\tau_{c\alpha}$. The imposed wave in this simulation has a negative phase velocity, as shown by the vertical dashed traces, and is in phase-space resonance with the α particles; these wave-particle interactions are visible in the asymmetry of the distribution functions around $v_x = 0$. The complex structure in Figs. 4(ii) and 4(iii) shows progression to the nonlinear phase.

In this Letter, we have identified a process whereby the effective energy confinement of the fusion-born α-particle population is significantly enhanced. As an externally applied fast Alfvén wave of initially low amplitude propagates inward, it is amplified by stimulated emission of energy from the α particles at the outer midplane, whose velocity distribution is inverted. This stimulated emission arises because this α-particle population is naturally linearly unstable to the MCI at the selected (ω, k) of the applied wave. We have measured the group velocity of the inward propagating wave to be $(-0.40 \pm 0.06)V_A$ and show that amplification occurs on a time scale $\sim 2\tau_{c\alpha}$–$5\tau_{c\alpha}$. Approximately half of the 10%–20% α-particle energy released is transferred inward to the fuel ions that support this wave, and the waves to which it couples, thereby leaving less free energy available for spontaneously excited waves that leave the plasma. The amplified wave passes into a nonlinear regime in which the background real space configuration—initially uniform—becomes modulated, resulting in wave packets traveling at nonidentical speeds. These are seen to collide, giving rise to increased phase-space complexity; this Letter does not investigate the spatial transport of α particles that accompanies energy exchange. The process reported here would be robust against turbulent transport effects due to the wide separation of time scales of these phenomena. This newly identified stimulated emission process is an instance of α-particle power channeling, which rests on velocity space resonance giving rise to real space energy transport towards the plasma core.

It is a pleasure to thank N. J. Fisch for the stimulating discussions. This work was partially funded by the Research

Councils UK Energy Programme (under Grant No. EP/I501045) and the European Communities. The views and opinions expressed herein do not necessarily reflect those of the European Commission. The EPOCH code used in this research was developed under U.K. Engineering and Physical Sciences Research Council Grants No. EP/G054940/1, No. EP/G055165/1, and No. EP/G056803/1.

*Corresponding author.
j.w.s.cook@warwick.ac.uk

[1] G. A. Cottrell and R. O. Dendy, Phys. Rev. Lett. **60**, 33 (1988).
[2] V. S. Belikov and Y. I. Kolesnichenko, Sov. Phys. Tech. Phys. **20**, 1146 (1976).
[3] R. O. Dendy, C. N. Lashmore-Davies, and K. F. Kam, Phys. Fluids B **4**, 3996 (1992).
[4] R. O. Dendy, C. N. Lashmore-Davies, and K. F. Kam, Phys. Fluids B **5**, 1937 (1993).
[5] R. O. Dendy, C. N. Lashmore-Davies, K. G. McClements, and G. A. Cottrell, Phys. Plasmas **1**, 1918 (1994).
[6] R. O. Dendy, K. G. McClements, C. N. Lashmore-Davies, R. Majeski, and S. Cauffman, Phys. Plasmas **1**, 3407 (1994).
[7] K. G. McClements, R. O. Dendy, C. N. Lashmore-Davies, G. A. Cottrell, S. Cauffman, and R. Majeski, Phys. Plasmas **3**, 543 (1996).
[8] R. O. Dendy, K. G. McClements, C. N. Lashmore-Davies, G. A. Cottrell, R. Majeski, and S. Cauffman, Nucl. Fusion **35**, 1733 (1995).
[9] N. N. Gorelenkov and C. Z. Cheng, Nucl. Fusion **35**, 1743 (1995).
[10] T. Fülöp and M. Lisak, Nucl. Fusion **38**, 761 (1998).
[11] G. A. Cottrell, V. P. Bhatnagar, O. Da Costa, R. O. Dendy, J. Jacquinot, K. G. McClements, D. C. McCune, M. F. F. Nave, P. Smeulders, and D. F. H. Start, Nucl. Fusion **33**, 1365 (1993).
[12] S. Cauffman, R. Majeski, K. G. McClements, and R. O. Dendy, Nucl. Fusion **35**, 1597 (1995).
[13] K. G. McClements, C. Hunt, R. O. Dendy, and G. A. Cottrell, Phys. Rev. Lett. **82**, 2099 (1999).
[14] J. Wesson, *Tokamaks*, 3rd ed. (Oxford University Press, New York, 2004).
[15] R. D'Inca *et al.*, in *Proceedings of the 38th EPS Conference on Plasma Physics, Strasbourg, France, 2011*, edited by A. Becoulet, T. Hoang, and U. Stroth (European Physical Society, Mulhouse, France, 2011), p. 1053.
[16] R. D'Inca, Ph.D. thesis, Max Planck Institute for Plasma Physics, 2013.
[17] M. Ichimura, H. Higaki, S. Kakimoto, Y. Yamaguchi, K. Nemoto, M. Katano, M. Ishikawa, S. Moriyama, and T. Suzuki, Nucl. Fusion **48**, 035012 (2008).
[18] S. Sato *et al.*, Plasma Fusion Res. **5**, S2067 (2010).
[19] G. Watson and W. W. Heidbrink, Rev. Sci. Instrum. **74**, 1605 (2003).
[20] W. W. Heidbrink *et al.*, Plasma Phys. Controlled Fusion **53**, 085028 (2011).
[21] K. Saito *et al.*, Plasma Sci. Technol. **15**, 209 (2013).
[22] J. W. S. Cook, R. O. Dendy, and S. C. Chapman, Plasma Phys. Controlled Fusion **55**, 065003 (2013).
[23] L. Carbajal, R. O. Dendy, S. C. Chapman, and J. W. S. Cook, Phys. Plasmas **21**, 012106 (2014).
[24] N. J. Fisch and J.-M. Rax, Phys. Rev. Lett. **69**, 612 (1992).
[25] N. J. Fisch, Phys. Plasmas **2**, 2375 (1995).
[26] M. C. Herrmann and N. J. Fisch, Phys. Rev. Lett. **79**, 1495 (1997).
[27] J. W. S. Cook, S. C. Chapman, and R. O. Dendy, Phys. Rev. Lett. **105**, 255003 (2010).
[28] J. W. S. Cook, S. C. Chapman, R. O. Dendy, and C. S. Brady, Plasma Phys. Controlled Fusion **53**, 065006 (2011).
[29] I. E. Ochs, N. Bertelli, and N. J. Fisch, Phys. Plasmas **22**, 082119 (2015).
[30] A. J. Fetterman and N. J. Fisch, Phys. Rev. Lett. **101**, 205003 (2008).
[31] A. I. Zhmoginov and N. J. Fisch, Phys. Rev. Lett. **107**, 175001 (2011).
[32] D. S. Clark and N. J. Fisch, Phys. Plasmas **7**, 2923 (2000).
[33] R. O. Dendy and K. G. McClements, Plasma Phys. Controlled Fusion **57**, 044002 (2015).
[34] K. G. McClements, R. D'Inca, R. O. Dendy, L. Carbajal, S. C. Chapman, J. W. S. Cook, R. W. Harvey, W. W. Heidbrink, and S. D. Pinches, Nucl. Fusion **55**, 043013 (2015).
[35] K. G. McClements and R. O. Dendy, J. Geophys. Res. **98**, 11689 (1993).
[36] R. O. Dendy and K. G. McClements, J. Geophys. Res. **98**, 15531 (1993).
[37] V. L. Rekaa, S. C. Chapman, and R. O. Dendy, Astrophys. J. **791**, 26 (2014).
[38] J. L. Posch, M. J. Engebretson, C. N. Olson, S. A. Thaller, A. W. Breneman, J. R. Wygant, S. A. Boardsen, C. A. Kletzing, C. W. Smith, and G. D. Reeves, J. Geophys. Res. **120**, 6230 (2015).
[39] N. J. Fisch, Rev. Mod. Phys. **59**, 175 (1987).
[40] T. H. Stix, *Waves in Plasmas* (Springer-Verlag, New York, 1992).
[41] T. D. Arber *et al.*, Plasma Phys. Controlled Fusion **57**, 113001 (2015).